Optimal Interception Technique Variation Calculus Task of Multidimensional Visual Ballistic Missiles

Umakant Bhaskrrao Gohatre, C. Ram Singla

Abstract: ***A strategy of manoeuvrating using inverted flight is presented to determine the optimal path for the dive stage of a hypersonic missile. The fighting incident in this document is taken into account when the hypersonic missile strikes the goal on the floor. In particular, the hypersonic rockets are first implemented by a maneuvering type called the reversed plane. The ideal route is later conceived by minimizing the attack time with the current terminal route angle, taking into consideration the limitations of the attack angle, fluid pressure, thermal transfer rate and ordinary overload. A better pseudo-spectral hp-adaptive technique with a mesh size decrease is introduced to resolve the constructed trajectory optimization issue. The paper shows the application of variation calculations in the process of anti-ballistic missile interception, to achieve the optimal concept of the open-switch control law. It provides analytical outcomes in the shape of suitable Euler-Lagrange Equations, relying on the preservation of the wind concept, for three distinct indices, using a simple racket and missile model. It also offers the computer program to simulate the intercom system quickly, with chosen parameters, parametrical assessment and simple alteration possibilities by other scientists, as published as m-Function of MATLAB in accessible code.***

Keywords: Projectile, Predictions, Variation calculus; optimal interception; ballistic rocket; optimal control

I. INTRODUCTION

Ballistic missile interception has been a subject of studies for years. Interception pathway calculation is normally carried out off-line using the two-point limit-value issue formulated. In the case of error trajectories in R6, the document [1] applies the suggested instruction scheme to: three NEDs (north-eastern-down), speed, route direction and projectile orientation, where error trajectories are attempted. Usually this requires the use of methods of optimization to achieve the paths of contact. There are four distinct instruction rules taken into consideration in [2] which show that the missile interception is feasible when the destination movements are perfectly measured and accurately estimated. To achieve the optimum entry level one can use a variety of methods, varying from the classical variation calculus as in this document to other methods, such as met heuristics, such as a genetic algorithm. Functional may apply to the interceptor's flight time or range from the ballistic missile. Guidance of a rocket interception is a multi-solution issue. Passive and aggressive methods can be distinguished [4]. Several kinds of effective instruction procedures may be differentiated: • a vision guideline (also called a bi-down guide), where the rocket intercepting is always directed towards the goal; · a deviant quest where the missile interception falls short of the goal; • proportional navigation, where the destination vision view range is measured;

Please apply to [9] for a more detailed perspective of the overall structure of a launcher and radar ballistic missile defense system. Another research can also be discovered in [10] on monitoring a ballistic missile.

For ages, methods of optimization were created, as mathematicians such as Leibnitz, Bernoulli and Newton of the Hospital advanced their own boundaries even further in the 17th Century. They are needed in production, in enterprise and/or in military applications, as everyone wants to collect the maximum possible amount in a shortest time, at the lowest possible cost and so on. The purpose of the present document is to use this strategy with the interception of an interceptor missile with a recognized path.

As already stated, an optimization approach in many areas is attractive and can include, for example, the quadratic cost function in an unrestricted problem, resulting in an easy solution. However, limitations are omnipresent in true life apps and must be considered during the phase of optimization. The optimization research is focused in this job on the variation calculus, e.g. described as the issue of discovering one that meets terminal circumstances between all ongoing x(t) functions[11]:

$$x(t_0) = x_0, x(t_f) = x_f, \tag{1}$$

Achieving local extreme of the functional

$$J(x) = \int_{t_0}^{t_f} f(f(t, x(t), \dot{x}(t))dt. \tag{2}$$

The latter job has solved terminal circumstances and the required continuity status of the Euler – Lagrange (E – L) matrix is fulfilled.

$$\frac{\partial f}{\partial x} - \frac{d}{dt}\left(\frac{\partial f}{\partial \dot{x}}\right) = 0. \tag{3}$$

From now on, the time indexes will be omitted where applicable without any misconceptions. For a initial variable point on the curve ¨(x), the x(t) function which crosses (t0,x0) and ¨(x) at times tf is sought. This feature meets the previous transversely requirements in relation to the E–L coefficient:

$$f(t_0, x, \dot{x}) = \left[(\dot{x}_0 - \dot{\phi})\frac{\partial f}{\partial \dot{x}}\right]\Big|_{t=t_0}, \tag{4}$$

Revised Manuscript Received on October 05, 2019.

***** Correspondence Author

Umakant Bhaskarrao Gohatre, Electronics and Communication Engineering Department, Madhav University, Pindwara, Rajasthan, India.
Email: umakantbhaskar@gmail.com

Dr. C. Ram Singla, Electronics and Communication Engineering Department, Madhav University, Pindwara, Rajasthan, India.
Email: Crslibra1010@gmail.com

The latter may include many methods, such as LQR[5] in the variation calculus structure and LQI (LQ Integrated) power law[6], which applies to linearized, predictive command and non-linear predictive monitoring schemes falling within the optimization strand[7], as well as PID setting performance-based approaches[8]. This document adopts the method of optimization, which generates the optimum open loop power message to minimize a certain efficiency coefficient at the required stage.

$$f(t_f, x, \dot{x}) = \left[(\dot{x}_0 - \dot{\phi})\frac{\partial f}{\partial \dot{x}}\right]\Big|_{t=t_f}. \quad (5)$$

If the feature relies onx−, the circumstances required as a collection of E–L variables are created. During the interception task, ć could indicate the route from the target to t0, or the path of the ship to be struck by tf, followed by the atomic column. Finally, when restrictions are available and can be in g–(t, x, u)=b–shape, where u indicates the power unit, and g–feature fulfills circumstances of consistency, feature can be placed in the following type.

$$J(x) = \int_{t_0}^{t_f} \left(f(t, x, \dot{x}, u, \dot{u}) + \underline{\lambda}^T \left(\underline{b} - \underline{g}(t, x, u) \right) \right) dt. \quad (6)$$

The above variation method is taken to obtain optimum command measurements for a missile, for which the model and parameters will be described in the next section. The anti-ballistic rocket is shortened as ABM and is generally a surface to air rocket intended to counteract ballistic rockets [12, 13].

This document introduces in open-text software that can not only simulates interception assignments, taking consideration in evaluation of multiple system parameters, but also to allow the ideal interception assignments to be resolved and regarded in the literature, introducing various situations and alternatives, but only as sheer outcomes and forms an in-depth domain of investigation. The primary motive and input of this job are to address all the problems in the article.

II. BALLISTIC ROCKET

A. Intercept Missile Models.

The issue of model precision should be discussed before providing a rocket model. Simplified intercepting missile design (1D) The most precise template is advantageous, but software calculations would take too long, and the mathematical explanation would deactivate any action. The model should be sufficiently streamlined to reflect, but not overly simpler, missile dynamics.

It is presumed that this missile moves in the reverse path with a power propulsion, where gasses from the rocket [14,15,16]. The momentum conservation principle, which says that the complete momentum of the rocket is used to allow mathematical depiction.

$$p_{\text{rocket}}(t) + p_{\text{gas}}(t) \quad (7)$$

$$p_{\text{gas}}(t) = mv(t), \quad (8)$$

M is the mass of the rocket, and v(t) is its speed. The impact of the drag is more difficult to quantify, however, because the drag-force is very small in many important applications. Potential drag effects in which air changes density at altitude usually lead to equations that can not be analytically integrated (digital integrations are required), and lead to a drag strength at level of 2 percent of the strength in typical flight conditions of a 12,000 kg rocket flying at 700 m/s.

The control system considered should function as follows: the control signal w(t) is a gas momentum, that gives the speed of the missile when divided by m. Integrating this speed, information on the racket position that is compared with the rocket trajectory information to be intercepted can be obtained. This position is measured by a sensor that is a pure feedback gain, which should be removed from the reference signal w in order to get an error of tracking. The controller itself is not required as an optimization results in the receipt of the open-loop control signal.

As far as the mar mass of the missile is concerned, k2 is the result of the internal feedback loop, w (t) is the reference signal (optimized control system input signal), and y(t) is the output of the missile, the following model is proposed.

$$k_1 = \frac{1}{m_r} \quad (9)$$

$$G(s) = \frac{Y(s)}{W(s)} = \frac{\frac{k_1}{s}}{1 + \frac{k_1 k_2}{s}} = \frac{\frac{1}{k_2}}{1 + \frac{1}{k_1 k_2} s} = \frac{k}{1 + sT}. \quad (10)$$

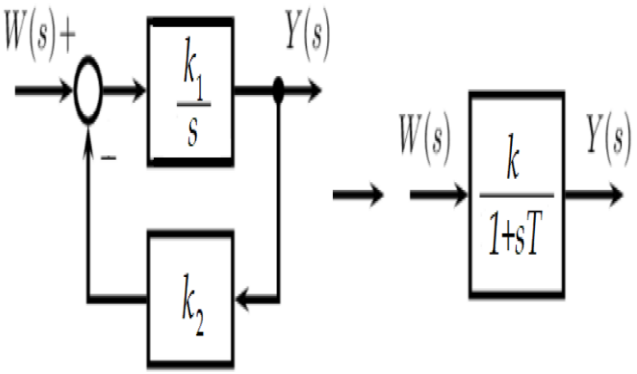

Fig. 1. Racket control system model

The rocket time constant is supposed to be some minutes, and its weight about 1000 kg [13, 17, 18]. Rocket control system model.

B. Approximately horizontally

The mid-phase of its flight is the typical ballistic rocket, which traces a parabolic function in the form of a so-called "tri-shape" function. The parabola should have a flat chart with a certain maximum assumption, such as 100 km in this paper. In Table 1 and Table 2[12], typical parameters of missile interception are given.

Table 1. Standard parameters of interception missiles.

Parameter	Value
maximum attitude	80 ÷ 100 km
linear velocity	2000 ÷ 6000 kmph
mass	1000 ÷ 10,000 kg
time of flight	20 ÷ 40 mins
range	100 ÷ 5000 km

Table 2. Selected parameters of sample interception missiles.

Parameter	Iskander	Shahab 3	MGM-31B Per/II
country	Russia	Iran	USA
mass	3800 kg	900 kg	7400 kg
max. vel.	6000 kmph	5500 kmph	3000 kmph
range	500 km	2100 km	1800 km

The trajectory of the rocket might be defined by the following canonical quadratic function

$$\varphi = a(t-p)^2 + q, \quad (11)$$

Where p[h] is the time when the rocket reaches its highest altitude, a shall be the incline and q[km] shall be the highest elevation[14,16].

The missile used to intercept the ballistic missile does not know when the rocket was launched, so t=0 indicates the launch time of the missile. If, for example, the default ballistic equation in 1D is assumed to be p=0.25hr with the arbitrary selection a=−10.

$$\varphi(t) = -10(t-0.25)^2 + 100. \quad (12)$$

This 1D case is a situation when the interception takes place directly over the site of interceptor rocket installation, below the expected trajectory of the ballistic missile.

C. The 2-Dimentional task:

Where the missile is being translated in two-dimensional spaces (distance versus altitude y), is the actual point of interest. The observer is assumed to be in parallel to the hyper plane on which the missile is translated and the rocket translated, and its observation angle, as described in Figure 2, is the right angle.

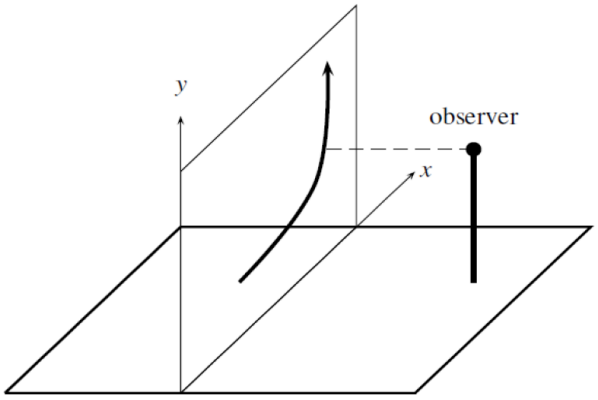

Fig. 2. Observer position.

By assuming a specified localization of the observer, there is no need to present the translation in 3D space, thus *z* axis information can be omitted.

Generalizing the previous 1D momentum equation to the 2D case [15],

$$p_{\text{total}} = m(v_x + v_y) = mv_x + mv_y = p_x + p_y, \quad (13)$$

Where velocity vector v– is decomposed into *x*- and *y*-components.

With the base vectors e–1 and e–2, the momentum

$$\underline{p} = p_x \underline{e}_1 + p_y \underline{e}_2 \quad (14)$$

D. Rocket Model (2D)

The ballistic rocket that should be intercepted is assumed to move as in the 1D case on a parabolic, and its range is assumed to be 2000 km by default and maximum height in y coordinate—100 km, i.e., it is a medium-range missile according to the American division or Russian classification [12], see Table 3 and Table 4.

Table 3. Type of missiles (US).

Range	Missile Type
150 ÷ 300 km	tactical ballistic missile
300 ÷ 1000 km	short-range ballistic missile
1000 ÷ 3500 km	medium-range ballistic missile
3500 ÷ 5500 km	intermediatet-range ballistic missile
over 5500 km	intercontinental ballistic missile

Table 4. Type of missiles (Russian).

Range	Missile Type
below 50 km	tactical missile
50 ÷ 300 km	operationa-tactial missile
300 ÷ 500 km	operational missile
500 ÷ 1000 km	operation-strategic missile
over 1000 km	strategic missile

Among American ABMs currently used one can find: MIM-104 Patriot (PAC-1 and PAC-2), U.S. Navy Aegis combat system using RIM-161 Standard Missile 3, or Russian Federation's missiles, as ABM-1 Galosh, ABM-3 Gazelle, ABM-4 Gorgon, and rockets of SAM system, like S-300P (SA-10) to S-400(SA-21).

As in the 1D case, a rocket is described in the canonical form of a quadratic equation along the Y axis.

$$\varphi_y(t) = a(t-p)^2 + q, \quad (15)$$

With the same description, whereas along the *x* axis as

$$\varphi_x(t) = gt, \quad (16)$$

Where g is the speed of the x-axis missile. As in the case of 2D, the plots shown here represent the interception phase during the mid-flight stage, in which the missile travel is relatively flat.

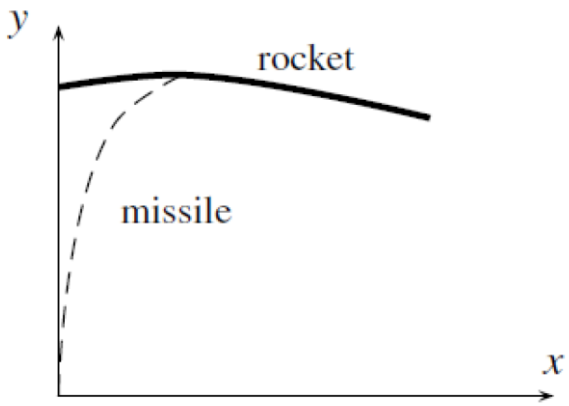

Fig. 3. Process of interception.

As with a 1D task, no information on its time of start is available to generate control action, so t=0 denotes the time of starting our missile, all flight parameters along the y-axis remain the same as in the 1D case. The g parameter is set to 400kmph by default.

The interception process is required when the ballistic rocket is descending, while the rocket is increasing its altitude continuously as shown in the Figure

III. PERFORMANCE INDICES:

Three performance indicators were considered in order to determine transversally conditions and to imitate different behaviors of the system.

It is always assumed that the optimal reference (input) w to the system is generated to make suitable changes inx, y and that a missile is intercepted. The following performance indicators refer to energy consumption or interception times, which have both clear meanings.

A. J1 Index

The first performance index refers to minimizing the energy from the input signals to the control system, as our control is based on an open-loop system and the issue is optimal input generation. In this event

$$J_1 = \int_{t_0}^{t_f} \left(w_x^2(t) + s w_y^2(t)\right) dt, \tag{17}$$

where *s* is the weight between the components. The input signal should satisfy dynamic equations of the rocket, and in both dimensions it should be the same, thus:

$$w_x = \frac{T}{k}\dot{x} + \frac{1}{k}x, \tag{18}$$

$$w_y = \frac{T}{k}\dot{y} + \frac{1}{k}y, \tag{19}$$

where wx denotes the position along the *x* axis, and wy along the *y* axis, *T* is a time constant, and *k* is the gain. The function under the integral takes the form:

$$f(t,x,\dot{x},y,\dot{y}) = \frac{T^2}{k^2}\dot{x}^2 + \frac{2T}{k^2}\dot{x}x + \frac{1}{k^2}x^2 + s\frac{T^2}{k^2}\dot{y}^2 + s\frac{2T}{k^2}\dot{y}y$$

Euler equations derivatives: $\frac{\partial f}{\partial x} = \frac{2T}{k^2}\dot{x} + \frac{2}{k^2}x,$ (20)

$$\frac{\partial f}{\partial \dot{x}} = \frac{2T^2}{k^2}\dot{x} + \frac{2T}{k^2}x, \tag{21}$$

$$\frac{d}{dt}\left(\frac{\partial f}{\partial \dot{x}}\right) = \frac{2T^2}{k^2}\ddot{x} + \frac{2T}{k^2}\dot{x}, \tag{22}$$

giving the E–L equation

$$T^2\ddot{x} - x = 0, \tag{23}$$

Which solution becomes $x(t) = C_1 exp^{-\frac{t}{T}} + C_2 exp^{\frac{t}{T}}$

By performing similar calculations in the *y* axis, one obtains

$$y(t) = C_3 exp^{-\frac{t}{T}} + C_4 exp^{\frac{t}{T}} \tag{24}$$

Since we have five unknowns (C1, C2, C3, C4, tf) the following boundary conditions must be used:

$$x(0) = 0,$$
$$x(t_k) = \varphi_x(t_k),$$
$$y(0) = 0,$$
$$y(t_k) = \varphi_y(t_k),$$
$$\left[(\dot{x} - \dot{\phi}_x)\frac{\partial f}{\partial \dot{x}}\right]\Big|_{t=t_k} + \left[(\dot{y} - \dot{\phi}_y)\frac{\partial f}{\partial \dot{y}}\right]\Big|_{t=t_k} = f(t_f). \tag{25}$$

Finally, a single equation is obtained

$$C_2^2 - gTC_2 exp^{\frac{t_f}{T}} + C_4^2 s - 2ag^2TC_4 st_f exp^{\frac{t_f}{T}} + 2ag^2TC_4 pse xp^{\frac{t_f}{T}} = \text{[illegible]}$$

B. Index J2

In the second performance index, only energy along the *y* axis is considered, since along the *x* axis the trajectory moves according to the linear equation of motion x=gt, thus

$$J_2 = \int_{t_0}^{t_f} w_y^2(t)dt, \tag{26}$$

Where

$$f(t,y,\dot{y}) = \frac{T^2}{k^2}\dot{y}^2 + \frac{2T}{k^2}\dot{y}y + \frac{1}{k^2}y^2. \tag{27}$$

By performing similar calculations as in the case of J1 one obtains the E–L equation

$$T^2\ddot{y} - y = 0, \tag{28}$$

The border conditions become: $y(0) = 0,$

$$y(t_f) = \varphi_y(t_f), \tag{29}$$

$$y(t) = C_1 exp^{-\frac{t}{T}} + C_2 exp^{\frac{t}{T}}\text{s} \tag{30}$$

$$\left[(\dot{y} - \dot{\phi}_y)\frac{\partial f}{\partial \dot{y}}\right]\Big|_{t=t_f} = f(t_f). \tag{31}$$

Finally, a single equation is obtained

$$2aTt_f\left(exp^{\frac{2t_f}{T}} - 1\right) + 2aTp\left(1 - exp^{\frac{2t_f}{T}}\right) = a(t_f - p)^2 + q.$$

C. Index J3

This index is connected to minimum-time control that requires the velocity constraint y˙=vmax to be introduced, otherwise the input command becomes infinite. The performance index is of the form

$$J_3 = \int_{t_0}^{t_f} dt. \tag{32}$$

There are no constraints imposed on the translation in *x* axis, since the movement in *x* axis is proportional to time

$$\varphi_x(t) = gt \tag{33}$$

thus minimum time implies minimal value of φx. Taking this constraint into consideration, the performance index takes the form

$$J_3 = \int_{t_0}^{t_f} (1 + \lambda(v_{\max} - \dot{y}))dt. \tag{34}$$

Euler equations derivatives for *y*:

$$\frac{\partial f}{\partial y} = 0,$$
$$\frac{\partial f}{\partial \dot{y}} = -\lambda,$$
$$\frac{d}{dt}\left(\frac{\partial f}{\partial \dot{y}}\right) = -\dot{\lambda},$$

And for λ:

$$\frac{\partial f}{\partial \lambda} = v_{\max} - \dot{y},$$
$$\frac{\partial f}{\partial \dot{\lambda}} = 0,$$
$$\frac{d}{dt}\left(\frac{\partial f}{\partial \dot{\lambda}}\right) = 0 \tag{35}$$

Yield in the following set of E–L equations:

$$\dot{\lambda} = 0,$$

With the solutions:

$$\dot{y} = v_{\max},$$
$$\lambda = C_1,$$
$$y = v_{\max}t + C_2. \tag{36}$$

Border conditions become:

$$y(0) = 0,$$
$$y(t_f) = \varphi_y(t_f), \tag{37}$$

And, as a result,

$$at_f^2 - (2ap + v_{max})t_f + ap^2 + q = 0. \quad (38)$$

From the latter equation, one can obtain the interception time. In the *x* axis, it is assumed that the equation of motion becomes

$$x(t) = C_3 exp^{-\frac{t}{T}} + C_4 exp^{\frac{t}{T}} \quad (39)$$

With border conditions

$$x(0) = 0,$$
$$x(t_f) = gt_f, \quad (40)$$

Where tf is already calculated for *y*

IV. SIMULATION PARAMETERS AND RESULTS

$$T = \frac{3.25}{60}\text{h}$$
$$p = 0.25\text{h}$$
$$k = 0.25$$
$$q = 100\text{km}$$
$$a = -10$$
$$g = 400\text{kmph}$$
$$h = 40\text{kmph}$$
$$v_{max} = 2500\text{kmph}$$
$$s = 0.00045\text{h}$$

It is to be stressed that parameter *s* has been chosen in such a way so as to obtain interception time in minutes, to avoid false results.

In all the considered interception problems, a single equation binding interception time has been obtained that needed to be solved, using numerical methods with sampling time ts=0.3s, resulting from observation of time constants of the obtained plots and on the basis of multiple simulations, and observations of performance indices behaviour

V. SIMULATION RESULTS

Below, the optimal curves for performance indices considered are included:

$$J_1^* = 1401$$
$$x^*(t) = -8.4274exp^{-\frac{t}{3.25}} + 8.4274exp^{\frac{t}{3.25}},$$
$$y^*(t) = -30.8138exp^{-\frac{t}{3.25}} + 30.8138exp^{\frac{t}{3.25}},$$
$$w_x^* = 67.40exp^{\frac{t}{3.25}},$$
$$w_y^* = 246.50exp^{\frac{t}{3.25}},$$
$$t_f = 4.0889\text{min};$$

(41)

$$J_2^* = 17,240$$
$$x^*(t) = 400t(\text{knowninadvance}),$$
$$y^*(t) = -1.3513exp^{-\frac{t}{3.25}} + 1.3513exp^{\frac{t}{3.25}},$$
$$w_y^* = 10.80exp^{\frac{t}{3.25}},$$
$$t_f = 13.9888\text{min};$$

(42)

$$J_3^* = 0.039$$
$$x^*(t) = -9.9156exp^{-\frac{t}{3.25}} + 9.9156exp^{\frac{t}{3.25}},$$
$$y^*(t) = 2500t,$$
$$w_x^* = 79.30exp^{\frac{t}{3.25}},$$
$$w_y^* = 1000t + 542,$$
$$t_f = 2.3894\text{min};$$

(43)

In Fig.4, Fig. 5 and Fig. 6, the visualization of the obtained results is presented in *y* axis, to show the interception takes place at the calculated time instants, whereas in Fig. 7, Fig. 8 and Fig. 9, the reference inputs are shown, respectfully.

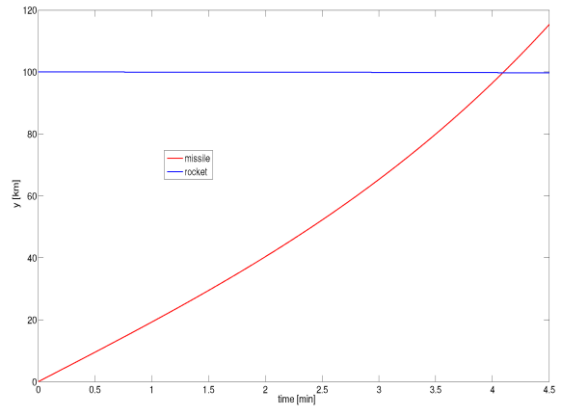

Fig. 4. Solution minimizing J1

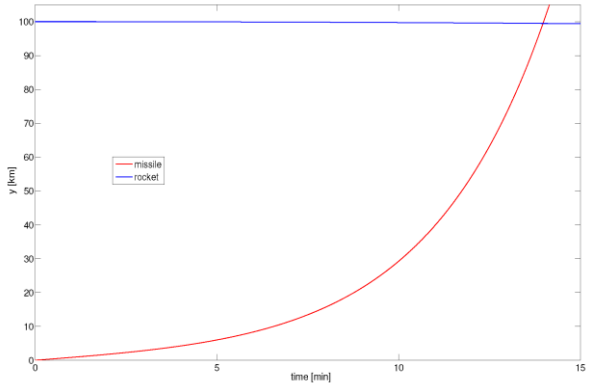

Fig. 5. Solution minimizing J2.

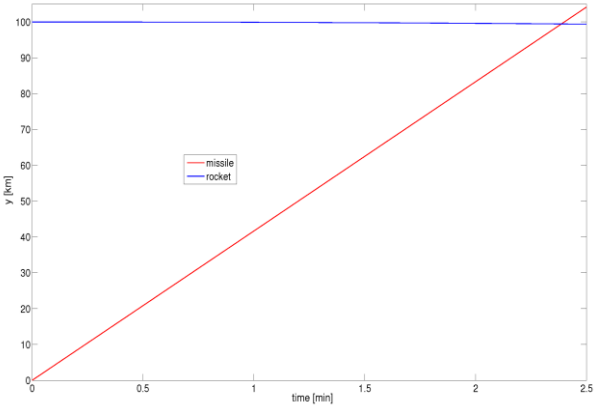

Fig. 6. Location Setup

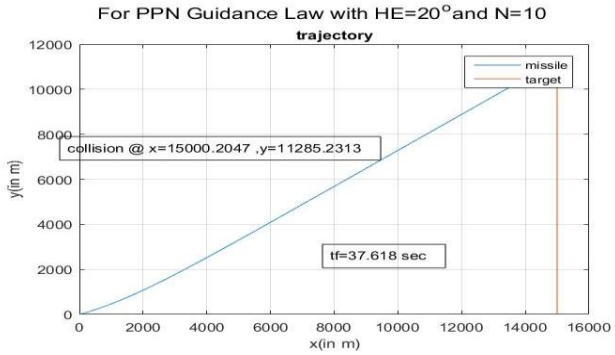

Fig. 7. PPN Guidence law HE=20 and N= 10

The software program with the GUI in Matlab has been created that solves using Symbolic Toolbox the equations defining interception time instants ft., calculates integration constants, and visualizes the results.

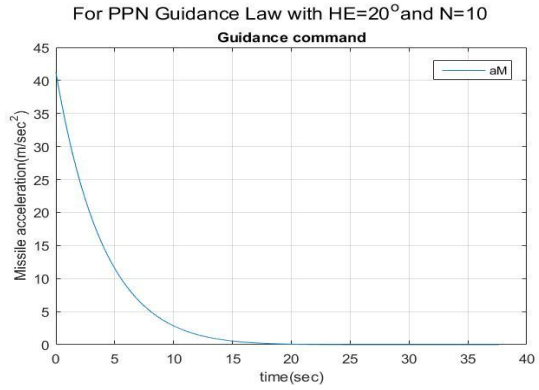

Fig.8. PPN Guidance command HE=20 and N= 10

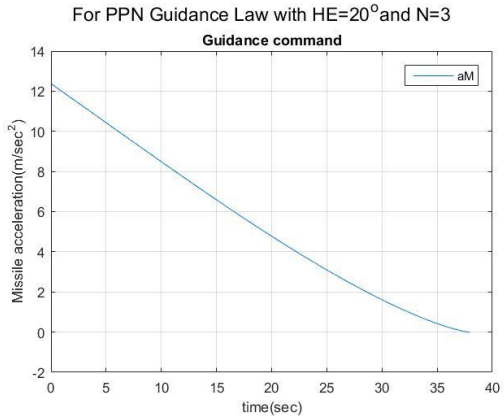

Fig.9. PPN Guidance command HE=20 and N=3

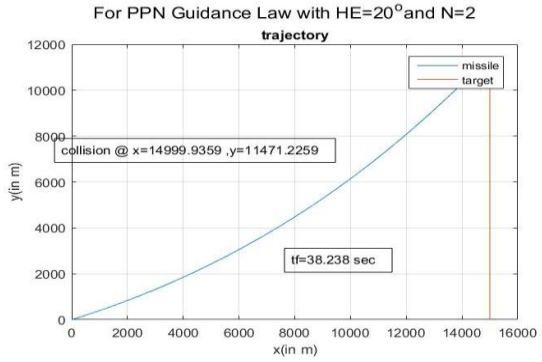

Fig.10. PPN Guidance command HE=20 and N=2

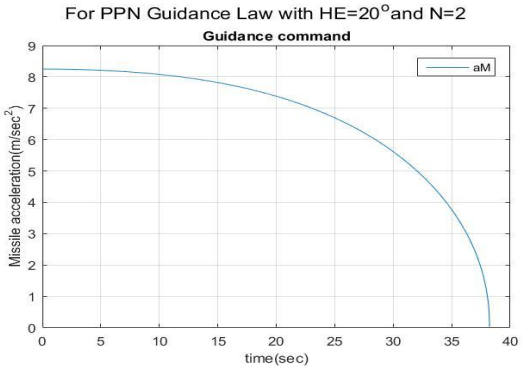

Fig.11. PPN Guidance command HE=20 and N=2

VI. CONCLUSION

The hypersonic rocket in the dive phase in this paper presents an optimal maneuvering trajectory. Compared to previous studies, the hypersonic missiles first receive a maneuver form called the inverted flight. In addition, an improved pseudo-spectral HI-adaptive approach with mesh size reduction is designed to solve the problem of trajectory optimization. Results of the simulations indicate that the suggested algorithm can decrease the mesh scale considerably with adequate precision, and comparison simulations verify the efficiency of the reversed plane. The work in this paper provides a maneuver strategy to break the enemy air defense system and maximize the target penetration for hypersonic missiles during a dive phases.

REFERENCES

1. Yakimenko, O.A.; Lukacs, J.A. Trajectory-Shaping Guidance for Interception of Ballistic Missiles during the Boost Phase. J. Guid. Control. Dyn. 2008, 31, 1524–1531. [Google Scholar] [CrossRef]
2. Shinar, J.; Zarkh, M. Interception of Maneuvering tactical ballistic missiles in the atmoshphere. In ICAS Proceedings; American INST of Aeronautics and Astronautics: Reston, VA, USA, 1994; pp. 1354–1363. [Google Scholar]
3. Yournas, I.; Aqeel, A. A Genetic algorithm for mid-air target interception. Int. J. Comput. Appl. 2011, 14, 38–42. [Google Scholar]
4. Yeboles, D.M. Analysis and Optimization of Trajectories for Ballistic Missles Interception. Ph.D. Thesis, Universidad Politechnica de Madrid, Madrid, Spain, 2015. [Google Scholar]
5. Owczarkowski, A.; Horla, D.; Zietkiewicz, J. Introduction of Feedback Linearization to Robust LQR and LQI Control—Analysis of Results from an Unmanned Bicycle Robot with Reaction Wheel. Asian J. Control. 2019, 21, 1028–1040. [Google Scholar] [CrossRef]
6. Owczarkowski, A.; Horla, D. Robust LQR and LQI control with actuator failure of a 2DOF unmanned bicycle robot stabilized by an interial wheel. Int. J. Appl. Math. Comput. Sci. 2016, 26, 325–334. [Google Scholar] [CrossRef]
7. Zietkiewicz, J. Nonlinear Predictive Control with Constraint Propagation Strategy. In Proceedings of the 18th International Conference on Mechatronics, Brno, Czech Republic, 5–7 December 2018; pp. 222–228. [Google Scholar]
8. Giernacki, W.; Sadalla, T. Comparison of Tracking Performance and Robustness of Simplified Models of Multirotor UAV's Propulsion Unit with CDM and PID Controllers. J. Control. Eng. Appl. Inform. 2017, 19, 31–40. [Google Scholar]
9. Na, H.; Lee, J.-I. Optimal Arrangement of Missile Defense Systems Considering Kill-Probability. In IEEE Transactions on Aerospace and Electronic Systems (Early Access); IEEE: Piscataway, NJ, USA, 2019. [Google Scholar]
10. Easthope, P.F. Probability of track impact in defended area: Use of Green's theorem in the plane. Studia z Automatyki i Informatyki 2018, 43, 65–72. [Google Scholar]
11. Gelfand, I.; Fomin, S. Calculus of Variations; Prentice Hall: Upper Saddle River, NJ, USA, 1963. [Google Scholar]
12. Ballistic Missile. Available online: https://en.wikipedia.org/wiki/Ballistic_missile (accessed on 15 April 2019)
13. Pietrasienski, J.; Warchulski, M.; Warchulski, J. Simulation Research on TBM's Shooting down by HIMAD SA-5 GAMMON AA system. Mechanik 2012, 85, 769–774. [Google Scholar]
14. Rocket and Space Technology. Basics of Space Flight: Rocket Propulsion. Available online: https://www.braeunig.us/space/propuls.htm (accessed on 20 March 2019).
15. Davis, D. Conservation of Momentum. Rocket Propulsion. Course 1351: General Physics I. Available online: https://www.ux1.eiu.edu/~cfadd/ 1350/09Mom/Rock.html (accessed on 20 April 2019).
16. HyperPhysics. Rocket Principles. Available online: http://hyperphysics.phy- astr.gsu.edu/ hbase/rocket.html (accessed on 15 May 2019).

17. 9K720 Iskander. Available online: https://en.wikipedia.org/wiki/9K720_ Iskander (accessed on 2 April 2019).
18. Mesko. The 120 mm Armor Piercing Fin Stabilized Discarding Sabot Tracer Target Practice (APFSDS-T-TP) for Rh 120 L44 Tank Gun. Available online: www.mesko.com.pl (accessed on 10 May 2019).
19. Giernacki, W.; Horla, D.; Sadalla, T. Mathematical models database (MMD ver. 1.0) non-commercial proposal for researchers. In Proceedings of the 21st International Conference on Methods and Models in Automation and Robotics, Miedzyzdroje, Poland, 29 August–1 September 2016; pp. 555–558.

AUTHORS PROFILE

Umakant Bhaskarrao Gohatre is graduated in **BE (ECE) and Master in VLSI and Embedded System Design** and is working as faculty of Engineering and Technology since 6 years under Engineering college of University of Mumbai affiliated college**s.** Currently working as Asst. Professor in Smt. Indira Gandhi Engineering College, Navi Mumbai since 6 years. His area of Research is Mathematical computational Models, Machine Learning, Image Processing, and Computer Vision. Currently he is research scholar ECE, Engineering Department, of Madhav University, Pindwara, and Rajasthan, India.

Dr. C. Ram Singla , 45+ Years of experience in the field of engineering education at various positions including Director, Principal, Advisor, HOD etc. Served various institutions of Haryana and Rajasthan and widely connected with educationists and technocrats all over India .First Ph.D. in the field of electronics engineering from MDU, Rohtak. Currently he is research Guide and HOD Electronics and Communication Engineering Department in Madhav University, Pindwara, Rajasthan.